Clifford M. Krowne
Yong Zhang
Editors

SPRINGER SERIES IN MATERIALS SCIENCE 98

Physics of Negative Refraction and Negative Index Materials

Optical and Electronic Aspects and Diversified Approaches

Springer

Springer Series in
MATERIALS SCIENCE 98

Springer Series in

MATERIALS SCIENCE

The Springer Series in Materials Science covers the complete spectrum of materials physics, including fundamental principles, physical properties, materials theory and design. Recognizing the increasing importance of materials science in future device technologies, the book titles in this series reflect the state-of-the-art in understanding and controlling the structure and properties of all important classes of materials.

Volumes 40–87 are listed at the end of the book.

C.M. Krowne Y. Zhang (Eds.)

Physics of Negative Refraction and Negative Index Materials

Optical and Electronic Aspects and Diversified Approaches

With 228 Figures

Springer

Dr. Clifford M. Krowne
Code 6851, Microwave Technology Branch
Electronics Science and Technology Division, Naval Research Laboratory
Washington, DC 20375-5347, USA
E-mail: krowne@webbsight.nrl.navy.mil

Dr. Yong Zhang
Materials Science Center, National Renewable Energy Laboratory (NREL)
1617 Cole Blvd., Golden, CO 80401, USA
E-mail: Yong_Zhang@nrel.gov

Series Editors:

ISSN 0933-033X

ISBN 978-3-540-72131-4 Springer Berlin Heidelberg New York

Library of Congress Control Number: 2007925169

Typesetting: Data prepared by SPI Kolam using a Springer TEX macro package
Cover: eStudio Calamar Steinen

Printed on acid-free paper SPIN: 11810377 57/3180/SPI 5 4 3 2 1 0

Preface

There are many potentially interesting phenomena that can be obtained with wave refraction in the "wrong" direction, what is commonly now referred to as negative refraction. All sorts of physically new operations and devices come to mind, such as new beam controlling components, reflectionless interfaces, flat lenses, higher quality lens or "super lenses," reversal of lenses action, new imaging components, redistribution of energy density in guided wave components, to name only a few of the possibilities. Negative index materials are generally, but not always associated with negative refracting materials, and have the added property of having the projection of the power flow or Poynting vector opposite to that of the propagation vector. This attribute enables the localized wave behavior on a subwavelength scale, not only inside lenses and in the near field outside of them, but also in principle in the far field of them, to have field reconstruction and localized enhancement, something not readily found in ordinary matter, referred to as positive index materials.

Often investigators have had to create, even when using positive index materials, interfaces based upon macroscopic or microscopic layers, or even heterostructure layers of materials, to obtain the field behavior they are seeking. For obtaining negative indices of refraction, microscopic inclusions in a host matrix material have been used anywhere from the photonic crystal regime all the way into the metamaterial regime. These regimes take one from the wavelength size on the order of the separation between inclusions to that where many inclusions are sampled by a wavelength of the electromagnetic field. Generally in photonic crystals and metamaterials, a Brillouin zone in reciprocal space exists due to the regular repetitive pattern of unit cells of inclusions, where each unit cell contains an arrangement of inclusions, in analogy to that seen in natural materials made up of atoms. Only here, the arrangements consist of artificial "atoms" constituting an artificial lattice.

The first two chapters of this book (Chaps. 1 and 2) address the use of uniform media to generate the negative refraction, and examine what happens

to optical waves in crystals, electron waves in heterostructures, and guided waves in bicrystals. The first chapter also contrasts the underlying physics in various approaches adopted or proposed for achieving negative refraction and examines the effects of anisotropy, as does the second chapter for negative index materials (left-handed materials). Obtaining left-handed material behavior by utilizing a permeability tensor modification employing magnetic material inclusions is investigated in Chap. 3. Effects of spatial dispersion in the permittivity tensor can be important to understanding excitonic–electromagnetic interactions (exciton–polaritons) and their ability to generate negative indices and negative refraction. This and other polariton issues are discussed in Chap. 4.

The next group of chapters, Chaps. 5 and 6, in the book looks at negative refraction in photonic crystals. This includes studying the effects in the microwave frequency regime on such lattices constructed as flat lenses or prisms, in two dimensional arrangements of inclusions, which may be of dielectric or metallic nature, immersed in a dielectric host medium, which could be air or vacuum. Even slight perturbations or crystalline disorder effects can be studied, as is done in Chap. 7 on quasi-crystals. Analogs to photonic fields do exist in mechanical systems, and Chap. 8 examines this area for acoustic fields which in the macroscopic sense are phonon fields on the large scale.

Finally, the last group of chapters investigates split ring resonator and wire unit cells to make metamaterials for creation of negative index materials. Chapter 9 does this as well as treating some of the range between metamaterials and photonic crystals by modeling and measuring split ring resonators and metallic disks. Chapter 10 looks at the effects of the split ring resonator and wire unit cells on left-handed guided wave propagation, finding very low loss frequency bands. Designing and fabricating split ring resonator and wire unit cells for lens applications is the topic of Chap. 11. This chapter has extensive modeling studies of various configurations of the elements and arrangements of their rectangular symmetry system lattice. The last chapter in this group and of the book, Chap. 12, delves into the area of nonlinear effects, expected with enhanced field densities in specific areas of the inclusions. For example, field densities may be orders of magnitude higher in the vicinity of the gaps in the split rings, than elsewhere, and it is here that a material could be pushed into its nonlinear regime.

The chapters here all report on recent research within the last few years, and it is expected that the many interesting fundamental scientific discoveries that have occurred and the applications which have resulted from them on negative index of refraction and negative index materials, will have a profound effect on the technology of the future. The contributors to this book prepared their chapters coming from very diversified backgrounds, and as such, provide the reader with unique perspectives toward the subject matter. Although the chapters are presented in the context of negative refraction and related

phenomena, the contributions should be found relevant to broad areas in fundamental physics and material science beyond the original context of the research. We expect this area to continue to yield new discoveries, applications, and insertion into devices and components as time progresses.

Washington and Golden, June 2007 *Clifford M. Krowne*
Yong Zhang

Contents

List of Contributors

Vladimir M. Agranovich
The University of Texas at Dallas
NanoTech Institute
Richardson, TX 75083-0688 USA

and

Institute of Spectroscopy
Russian Academy of Sciences
Troitsk, Moscow obl. 142190, Russia
vladimir.agranovich@utdallas.edu

Che Ting Chan
Physics Department
Hong Kong University of Science
and Technology
Clear Water Bay, Hong Kong, China
phchan@ust.hk

Bingying Cheng
Institute of Physics
Chinese Academy of Sciences
Beijing 100080

Siu-Tat Chui
Department of Physics
and Astronomy
University of Delaware
Newark, DE 19716, USA
chui@bartol.udel.edu

Zhifang Feng
Institute of Physics
Chinese Academy of Sciences
Beijing 100080

K.H. Fung
Physics Department
Hong Kong University of Science
and Technology
Clear Water Bay, Hong Kong, China

Yuri N. Gartstein
Department of Physics
The University of Texas at Dallas
Richardson, Texas 75083, USA

Robert B. Greegor
Boeing Phantom Works
Seattle, WA 98124
Robert.b.greegor@boeing.com

L.B. Hu
Bartol Research Institute
and Department of Physics
and Astronomy
University of Delaware
Newark, DE 19711, USA

Yuri S. Kivshar
Nonlinear Physics Centre and Center for Ultra-High Bandwidth Devices for Optical Systems (CUDOS)
Research School of Physical Sciences and Engineering
Australian National University
Canberra, ACT 0200, Australia
ysk@internode.on.net

Clifford M. Krowne
Microwave Technology Branch
Electronics Science and Technology Division
Naval Research Laboratory
Washington, DC 20375-5347
krowne@webbsight.nrl.navy.mil

Jensen Li
Physics Department
Hong Kong University of Science and Technology
Clear Water Bay, Hong Kong, China

Zhi-Yuan Li
Institute of Physics
Chinese Academy of Sciences
Beijing 100080

Zifang Lin
Bartol Research Institute
and Department of Physics and Astronomy
University of Delaware
Newark, DE 19711, USA

Z.Y. Liu
Physics Department
Wuhan University
Wuhan, China

Peter F. Loschialpo
Naval Research Laboratory
Washington, DC 20375

Wentao Lu
Department of Physics
and Electronic Materials Research Institute
Northeastern University
Boston, MA 02115, USA
w.lu@neu.edu

Angelo Mascarenhas
Materials Science Center
National Renewable Energy Laboratory (NREL)
1617 Cole Blvd.
Golden, CO 80401, USA

Ekmel Ozbay
Nanotechnology Research Center
Department of Physics
and Department of Electrical and Electronics Engineering
Bilkent University
Bilkent, 06800 Ankara, Turkey
ozbay@bilkent.edu.tr

Gonca Ozkan
Nanotechnology Research Center
Bilkent University
Bilkent 06800, Ankara, Turkey

Claudio G. Parazzoli
Boeing Phantom Works
Seattle, WA 98124

Frederic Rachford
Material Science and Technology Division
Naval Research Laboratory
Washington, DC 20375
rachford@anvil.nrl.navy.mil

Ilya V. Shadrivov
Nonlinear Physics Centre
Research School of Physical Sciences and Engineering
Australian National University
Canberra ACT 0200, Australia

Ping Sheng
Physics Department
Hong Kong University of Science
and Technology
Clear Water Bay, Hong Kong, China

Douglas L. Smith
Naval Research Laboratory
Washington, DC 20375

Srinivas Sridhar
Vice Provost for Research
Director, Electronic Materials
Research Institute
Arts and Sciences Distinguished
Professor of Physics
Northeastern University
360 Huntington Avenue,
Boston, MA 02115, USA
ssridhar@neu.edu

Minas H. Tanielian
Boeing Phantom Works
Seattle, WA 98124

P. Vodo
Department of Physics
and Electronic Materials
Research Institute
Northeastern University
Boston, MA 02115, USA

Yiquan Wang
Institute of Physics
Chinese Academy of Sciences
Beijing 100080

Dao-Zhong Zhang
Institute of Physics
Chinese Academy of Sciences
Beijing 100080

Xiangdong Zhang
Beijing Normal University
Beijing 100875, China
zhangxd@bnu.edu.cn

Yong Zhang
Materials Science Center
National Renewable Energy
Laboratory (NREL)
1617 Cole Blvd.
Golden, CO 80401
Yong_Zhang@nrel.gov

Lei Zhou
Bartol Research Institute
and Department of Physics
and Astronomy
University of Delaware
Newark, DE 19711, USA

1

Negative Refraction of Electromagnetic and Electronic Waves in Uniform Media

Y. Zhang and A. Mascarenhas

Summary. We discuss various schemes that have been used to realize negative refraction and zero reflection, and the underlying physics that dictates each scheme. The requirements for achieving both negative refraction and zero reflection are explicitly given for different arrangements of the material interface and different structures of the electric permittivity tensor $\boldsymbol{\varepsilon}$. We point out that having a left-handed medium is neither necessary nor sufficient for achieving negative refraction. The fundamental limitations are discussed for using these schemes to construct a perfect lens or "superlens," which is the primary context of the current interest in this field. The ability of an ideal "superlens" beyond diffraction-limit "focusing" is contrasted with that of a conventional lens or an immersion lens.

1.1 Introduction

1.1.1 Negative Refraction

Recently, negative refraction has attracted a great deal of attention, largely due to the realization that this phenomenon could lead to the development of a perfect lens (or superlens) [1]. A perfect lens is supposed to be able to focus all Fourier components (i.e., the propagating and evanescent modes) of a two-dimensional (2D) image without missing any details or losing any energy. Although such a lens has yet to be shown possible either physically and practically, the interest has generated considerable research in electromagnetism and various interdisciplinary areas in terms of fundamental physics and material sciences [2–4]. Negative refraction, as a physical phenomenon, may have much broader implications than making a perfect lens. Negative refraction achieved using different approaches may involve very different physics and may find unique applications in different technology areas. This chapter intends to offer some general discussion that distinguishes the underlying physics of various approaches, bridges the physics of different disciplines (e.g., electromagnetism and electronic properties of the material), and provides some detailed discussions for one particular approach, that is, negative

refraction involving uniform media with conventional dielectric properties. By uniform medium we mean that other than the microscopic variation on the atomic or molecular scale the material is spatially homogeneous.

The concept of negative refraction was discussed as far back as 1904 by Schuster in his book *An Introduction to the Theory of Optics* [5]. He indicated that negative dispersion of the refractive index, n, with respect to the wavelength of light, λ, i.e., $\mathrm{d}n/\mathrm{d}\lambda < 0$, could lead to negative refraction when light enters such a material (from vacuum), and the group velocity, v_g, is in the opposite direction to the wave (or phase) velocity, v_p. Although materials with $\mathrm{d}n/\mathrm{d}\lambda < 0$ were known to exist even then (e.g., sodium vapor), Schuster stated that "in all optical media where the direction of the dispersion is reversed, there is a very powerful absorption, so that only thicknesses of the absorbing medium can be used which are smaller than a wavelength of light. Under these circumstances it is doubtful how far the above results have any application." With the advances in material sciences, researchers are now much more optimistic 100 years later. Much of the intense effort in demonstrating a "poor man's" superlens is directed toward trying to overcome Schuster's pessimistic view by using the spectral region normally having strong absorption and/or thin-film materials with film thicknesses in the order of (or even a fraction of) the wavelength of light [2]. However, with regard to the physics of refraction, for a "lens" of such thickness, one may not be well justified in viewing the transmission as refraction, because of various complications (e.g., the ambiguity in defining the layer parameters [6] and the optical tunnel effect [7]).

The group velocity of a wave, $\mathbf{v}_\mathrm{g}(\omega, \mathbf{k}) = \mathrm{d}\omega/\mathrm{d}\mathbf{k}$, is often used to describe the direction and the speed of its energy propagation. For an electromagnetic wave, strictly speaking, the energy propagation is determined by the Poynting vector $\mathbf{S}$. In certain extreme situations, the directions of $\mathbf{v}_\mathrm{g}$ and $\mathbf{S}$ could even be reversed [8]. However, for a quasimonochromatic wave packet in a medium without external sources and with minimal distortion and absorption, the direction of $\mathbf{S}$ does coincide with that of $\mathbf{v}_\mathrm{g}$ [9]. For simplicity, we will focus on the simpler case, where the angle between $\mathbf{v}_\mathrm{g}$ and wave vector $\mathbf{k}$ is of significance in distinguishing two types of media: when the angle is acute or $\mathbf{k} \cdot \mathbf{v}_\mathrm{g} > 0$, it is said to be a right-handed medium (RHM); when the angle is obtuse or $\mathbf{k} \cdot \mathbf{v}_\mathrm{g} < 0$, it is said to be a left-handed medium (LHM) [10]. If one prefers to define the direction of the energy flow to be positive, an LHM can be referred to as a material with a negative wave velocity, as Schuster did in his book. A wave with $\mathbf{k} \cdot \mathbf{v}_\mathrm{g} < 0$ is also referred to as a backward wave (with negative group velocity), in that the direction of the energy flow is opposite to that of the wave determined by $\mathbf{k}$ [11, 12]. Lamb was perhaps the first to suggest a one-dimensional mechanical device that could support a wave with a negative wave velocity [13], as mentioned in Schuster book [5]. Examples of experimental demonstrations of backward waves can be found in other review papers [4, 14]. Unusual physical phenomena are expected to emerge either in an individual LHM (e.g., a reversal of the group velocity and a reversal of Doppler shift) or jointly with an RHM (e.g., negative refraction that occurs

at the interface of an LHM and RHM) [10]. The effect that has received most attention lately is the negative refraction at the interface of an RHM and LHM, which relies on the property $\mathbf{k} \cdot \mathbf{v}_\mathrm{g} < 0$ in the LHM.

There are a number of ways to realize negative refraction [4]. Most ways rely on the above-mentioned LH behavior, i.e., $\mathbf{k} \cdot \mathbf{v}_\mathrm{g} < 0$, although LH behavior is by no means necessary or even sufficient to have negative refraction. Actually, LH behavior can be readily found for various types of wave phenomena in crystals. Examples may include the negative dispersion of frequency $\omega(\mathbf{k})$ for phonons and of energy $E(\mathbf{k})$ for electrons; however, they are inappropriate to be considered as uniform media and thus to discuss refraction in the genuine sense, because the wave propagation in such media is diffractive in nature. For a simple electromagnetic wave, it is not trivial to find a crystal that exhibits LH behavior. By "simple electromagnetic wave," we refer to the electromagnetic wave in the transparent spectral region away from the resonant frequency of any elementary excitation in the crystal. In this case, the light–matter interaction is mainly manifested as a simple dielectric function $\varepsilon(\omega)$, as in the situation often discussed in crystal optics [15], where $\varepsilon(\omega)$ is independent of $\mathbf{k}$.

1.1.2 Negative Refraction with Spatial Dispersion

The first scheme to be discussed for achieving negative refraction relies on the $\mathbf{k}$ dependence of ε to produce the LH behavior. The dependence of $\varepsilon(\mathbf{k})$ or $n(\lambda)$ is generally referred to as spatial dispersion [16, 17], meaning that the dielectric parameter varies spatially. Thus, this scheme may be called the *spatial-dispersion scheme*. The negative refraction originally discussed by Schuster in 1904 could be considered belonging to this scheme, although the concept of spatial dispersion was only introduced later [17] and discussed in greater detail in a book by Agranovich and Ginzburg, *Spatial Dispersion in Crystal Optics and the Theory of Excitons* [9]. If one defines $v_\mathrm{p} = \omega/k = c/n$, and assumes $n > 0$, then according to Schuster, v_g is related to v_p by [5]

$$v_\mathrm{g} = v_\mathrm{p} - \lambda \frac{\mathrm{d}v_\mathrm{p}}{\mathrm{d}\lambda}, \tag{1.1}$$

and the condition for having a negative wave velocity is given as $\lambda\, \mathrm{d}v_\mathrm{p}/\mathrm{d}\lambda > v_\mathrm{p}$, which is equivalent to $\mathrm{d}n/\mathrm{d}\lambda < -n/\lambda < 0$. Negative group velocity and negative refraction were specifically associated with spatial dispersion by Ginzburg and Agranovich [9, 17]. Recently, a generalized version of this condition has been given by Agranovich et al. [18]. In their three-fields $(\mathbf{E}, \mathbf{D}, \mathbf{B})$ approach, with a generalized permittivity tensor $\tilde{\varepsilon}(\omega, \mathbf{k})$ (see the chapter of Agranovich and Gartstein for more details), the time-averaged Poynting vector in an isotropic medium is given as

$$\mathbf{S} = \frac{c}{8\pi}\mathrm{Re}(\mathbf{E}^* x \mathbf{B}) - \frac{\omega}{16\pi}\nabla_k \tilde{\varepsilon}(\omega, \mathbf{k})\mathbf{E}^*\mathbf{E}, \tag{1.2}$$

where the direction of the first term coincides with that of $\mathbf{k}$, and that of the second term depends on the sign of $\nabla_{\mathrm{k}}\tilde{\varepsilon}(\omega, \mathbf{k})$, which could lead to the reversal of the direction of $\mathbf{S}$ with respect to $\mathbf{k}$ under certain conditions. If permeability $\mu = 1$ is assumed, the condition can be simplified to $\mathrm{d}\varepsilon/\mathrm{d}k > 2\varepsilon/k > 0$ (here, ε is the conventional permittivity or dielectric constant), which is essentially the same as that derived from (1.1). Spatial dispersion is normally very weak in a crystal, because it is characterized by a parameter a/λ, where a is the lattice constant of the crystal and λ is the wavelength in the medium. However, when the photon energy is near that of an elementary excitation (e.g., exciton, phonon, or plasmon) of the medium, the light–matter interaction can be so strong that the wave is neither pure electromagnetic nor electronic, but generally termed as a polariton [19, 20]. Thus, the spatial dispersion is strongly enhanced, as a result of coupling of two types of waves that normally belong to two very different physical scales. With the help of the polariton effect and the negative exciton dispersion $\mathrm{d}E(\mathbf{k})/\mathrm{d}k < 0$, one could, in principle, realize negative refraction for the polariton wave inside a crystal if the damping is not too strong [21]. Because damping or dissipation is inevitable near the resonance, similar to the case of sodium vapor noted by Schuster [5], a perfect lens is practically impossible with this *spatial-dispersion scheme*.

It is worth mentioning that the damping could actually provide another possibility to induce $\mathbf{k} \cdot \mathbf{v}_{\mathrm{g}} < 0$ for the polariton wave in a crystal, even though in such a case the direction of $\mathbf{v}_{\mathrm{g}}$ may not be exactly the same as that of $\mathbf{S}$. In the *spatial-dispersion scheme*, the need to have $\mathrm{d}E(\mathbf{k})/\mathrm{d}k < 0$ is based on the assumption of the ideal polariton model, i.e., with vanishing damping. However, with finite damping, even with the electronic dispersion $\mathrm{d}E(\mathbf{k})/\mathrm{d}k > 0$, one may still have one polariton branch exhibiting $\mathrm{d}\omega/\mathrm{d}\mathbf{k} < 0$ near the frequency window Δ_{LT}, splitting the longitudinal and transverse mode, and thus, causing the exhibiting of LH behavior [7].

1.1.3 Negative Refraction with Double Negativity

Mathematically, the simplest way to produce LH behavior in a medium is to have both $\varepsilon < 0$ and $\mu < 0$, as pointed out by Pafomov [22]. Double negativity, by requiring energy to flow away from the interface and into the medium, also naturally leads to a negative refractive index $n = -\sqrt{\varepsilon\mu}$, thus facilitating negative refraction at the interface with an RHM, as discussed by Veselago [10]. At first glance, this *double-negativity scheme* would seem to be more straightforward than the *spatial-dispersion scheme*. However, $\varepsilon < 0$ is only known to occur near the resonant frequency of a polariton (e.g., plasmon, optical phonon, exciton). Without damping and spatial dispersion, the spectral region of $\varepsilon < 0$ is totally reflective for materials with $\mu > 0$. $\mu < 0$ is also known to exist near magnetic resonances, but is not known to occur in the same material and the same frequency region where $\varepsilon < 0$ is found. Indeed, if in the same material and spectral region one could simultaneously have $\varepsilon < 0$ and $\mu < 0$ yet without any dissipation, the material would then turn

transparent. In recent years, metamaterials have been developed to extend material response and thus allow effective ε and μ to be negative in an overlapped frequency region [3]. The hybridization of the metamaterials with, respectively, $\varepsilon_{\text{eff}} < 0$ and $\mu_{\text{eff}} < 0$ has made it possible to realize double negativity or $n_{\text{eff}} < 0$ in a small microwave-frequency window, and to demonstrate negative refraction successfully [23]. However, damping or dissipation near the resonant frequency still remains a major obstacle for practical applications of metamaterials. There is a fundamental challenge to find any natural material with nonunity μ at optical frequencies or higher, because of the ambiguity in defying μ at such frequencies [18,24]. Although there have been a few demonstrations of metamaterials composed of "artificial atoms" exhibiting nonunity or even negative effective μ and negative effective refractive index at optical frequencies [25–29], no explicit demonstration of negative refraction or imaging has been reported, presumably because of the relative large loss existed in such materials. Thus, the *double-negativity scheme* essentially faces the same challenge that the *spatial-dispersion scheme* does in realizing the dream of making a perfect lens.

1.1.4 Negative Refraction Without Left-Handed Behavior

It is perhaps understandable that the general public might have the impression that negative refraction never occurs in nature [23,30]. One could only make such a claim if one insists on using isotropic media [4,31,32]. The simplest example of negative refraction is perhaps refraction of light at the interface of air and an anisotropic crystal without any negative components of ε and μ, as illustrated in Fig. 1.1 [32–36]. A standard application of such an optical component is a beam displacer. Thus, negative refraction is a readily observable phenomenon, if one simply allows the use of an anisotropic medium. This *anisotropy scheme* has enabled the demonstration of negative refraction in the most genuine sense – that is, the classic refraction phenomenon in uniform media or optical crystals in a broad spectral range and involving neither electronic nor magnetic resonances [31,34,35]. As in the case of the double-negativity scheme, to eliminate the reflection at the medium interface, the *anisotropy scheme* also needs to satisfy certain conditions for matching the dielectric properties of the two media, as illustrated by a special case of a bicrystal structure [31]. In general, eliminating the reflection loss requires material parameters to automatically ensure the continuity of the energy flux

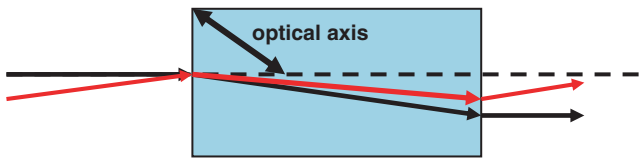

Fig. 1.1. Refraction of light at the interface of air and a (positive) uniaxial crystal

along the interface normal [32]. Generalization has been discussed for the interface of two arbitrary uniaxially anisotropic media [33, 37, 38]. Note that negative refraction facilitated by the anisotropy scheme does not involve any LH behavior and thus cannot be used to make a flat lens, in contrast to that suggested by Veselago, using a double-negativity medium [10], which is an important distinction from the other schemes based on negative group velocity. However, one could certainly envision various important applications other than the flat lens.

1.1.5 Negative Refraction Using Photonic Crystals

The last scheme we would like to mention is the *photonic crystal scheme*. Although it is diffractive in nature, one may often consider the electromagnetic waves in a photonic crystal as waves with new dispersion relations, $\omega_n(\mathbf{k})$, where n is the band index, and $\mathbf{k}$ is the wave vector in the first Brillouin zone. For a three-dimensional (3D) or 2D photonic crystal [39, 40], the direction of the energy flux, averaged over the unit cell, is determined by the group velocity $\mathrm{d}\omega_n(\mathbf{k})/\mathrm{d}\mathbf{k}$, although that might not be generally true for a 1D photonic crystal [40]. If the dispersion is isotropic, the condition $\mathbf{q}\cdot \mathrm{d}\omega_n(\mathbf{q})/\mathrm{d}\mathbf{q} < 0$, where $\mathbf{q}$ is the wave vector measured from a local extremum, must be satisfied to have LH behavior. Similar to the situations for the spatial-dispersion and double-negativity schemes, $\mathbf{q}\cdot \mathrm{d}\omega_n(\mathbf{q})/\mathrm{d}\mathbf{q} < 0$ also allows the occurrence of negative refraction at the interface of air and photonic crystal as well as the imaging effect with a flat photonic slab [4, 41–44]. However, similar to the situation for the anisotropy scheme, one may also achieve negative refraction with positive, but anisotropic, dispersions [40]. Because of the diffractive nature, the phase matching at the interface of the photonic crystal often leads to complications, such as the excitation of multiple beams [40, 45].

1.1.6 From Negative Refraction to Perfect Lens

Although the possibility of making a flat lens with the double-negativity material was first discussed by Veselago [10], the noted unusual feature alone, i.e., a lens without an optical axis, would not have caused it to receive such broad interest. It was Pendry who suggested perhaps the most unique aspect of the double-negativity material – the potential for realizing a perfect lens beyond negative refraction [1] – compared to other schemes that can also achieve negative refraction. Apparently, not all negative refractions are equal. To make Pendry's perfect lens, in addition to negative refraction, one also needs (1) zero dissipation, (2) amplification of evanescent waves, and (3) matching of the dielectric parameters between the lens and air. Exactly zero dissipation is physically impossible for any real material. For an insulator with an optical bandgap, one normally considers that there is no absorption for light with energy below the bandgap, if the crystal is perfect (e.g., free of defects). However, with nonlinear optical effects taken into account, there will

always be some finite absorption below the bandgap due to harmonic transitions [46]. Although it is typically many orders of magnitude weaker than the above-bandgap linear absorption, it will certainly make the lens imperfect. Therefore, a perfect lens may simply be a physically unreachable singularity point. For the schemes working near the resonant frequencies of one kind or the other, the dissipation is usually strong, and thus more problematic to allow such a lens to be practically usable.

Mathematically, double-negativity material is the only one, among all the schemes mentioned above, that automatically provides a correct amount of amplification for each evanescent wave [1]. Unfortunately, this scheme becomes problematic at high frequencies because of the ambiguity in defining nonunity μ at high frequencies [18, 24]. The other schemes – spatial dispersion and photonic crystals – may also amplify the evanescent components when the effective refractive index $n_{\text{eff}} < 0$, but typically with some complications (e.g., the amplification magnitude might not be exactly correct or the resolution is limited by the periodicity of the photonic crystal) [47, 48].

One important requirement of negative refraction for making a perfect lens is matching the dielectric parameters ("impedances") of the two media to eliminate reflection, as well as aberration [49], for instance, $n_1 = -n_2$ for the double-negativity scheme. In addition to the limitation caused by finite damping, another limitation faced by both the spatial-dispersion and double-negativity schemes is frequency dispersion, which prohibits the matching condition of the dielectric parameters to remain valid in a broad frequency range. For the spatial-dispersion scheme, the frequency dispersion $\varepsilon(\omega)$ is apparent [9]. It is less trivial for the double-negativity scheme, but it was pointed out by Veselago that "the simultaneous negative values of ε and μ can be realized only when there is frequency dispersion," in order to avoid the energy becoming negative [10]. For the photonic crystal, the effective index is also found to depend on frequency. Therefore, even for the ideal case of vanishing damping, the matching condition can be found at best for discrete frequencies, using any one of the three schemes discussed above.

However, even with the practical limitations on the three aspects – damping, incorrect magnitude of amplification, and dielectric mismatch – one can still be hopeful of achieving a finite improvement in "focusing" light beyond the usual diffraction limit [50], in addition to the benefits of having a flat lens. A widely used technique, an immersion lens [51], relies on turning as many evanescent waves as possible into propagating waves inside the lens, and it requires either the source or image to be in the near-field region. Compared to this immersion lens, the primary advantage of the "superlens" seems to be the ability to achieve subwavelength focusing with both the source and image at far field. An immersion lens can readily achieve $\sim \lambda/4$ resolution at $\sim$200 nm in semiconductor photolithography [52]. With a solid immersion lens, even better resolution has been achieved (e.g., $\sim 0.23\lambda$ at $\lambda = 436$ nm [53], $\sim\lambda/8$ at $\lambda = 515$ nm [54]). Thus far, using negative refraction, there have only been a few experimental demonstrations of non-near-field imaging with

improved resolution (e.g., 0.4λ image size at 1.4λ away from the lens [55], using a 2D quasicrystal with $\lambda = 25\,\text{mm}$; 0.36λ image size at 0.6λ away from the lens [56], using a 3D photonic crystal with $\lambda = 18.3\,\text{mm}$). In addition, plasmonic systems (e.g., ultra thin metal film) have also be used for achieving subwavelength imaging in near field [57, 58], although not necessarily related to negative refraction.

Some further discussion is useful on the meaning of "focusing" as used by Pendry for describing the perfect lens [1]. The focusing power of a lens usually refers to the ability to provide an image smaller than the object. What the hypothetical flat lens can do is exactly reproduce the source at the image site, or equivalently, spatially translate the source by a distance of $2d$, where d is the thickness of the slab. Thus, mathematically, a δ-function source will give rise to a δ-function image, without being subjected to the diffraction limit of a regular lens, i.e., $\lambda/2$ [59]. And such a "superlens" can, in principle, resolve two objects with any nonzero separation, overcoming the Rayleigh criterion of 0.61λ for the resolving power of a regular lens [59]. However, what this "superlens" cannot do is focus an object greater than λ to an image smaller than λ; thus, it cannot bring a broad beam to focus for applications such as photolithography, whereas a regular lens or an immersion lens can, in principle, focus an object down to the diffraction limit $\lambda/2$ or $\lambda/(2n)$ (n is the refractive index of the lens material). Therefore, it might not be appropriate to call such optical device of no magnification a "lens," though it is indeed very unique. One could envision using the "superlens" to map or effectively translate a light source, while retaining its size that is already below the diffraction limit to begin with.

1.2 Conditions for Realizing Negative Refraction and Zero Reflection

Let us consider a fairly general case of refraction of light at the interface of two uniform media, as shown in Fig. 1.2. The media are assumed to have anisotropic permittivity tensors ε_{L} and ε_{R}, both with uniaxial symmetry,

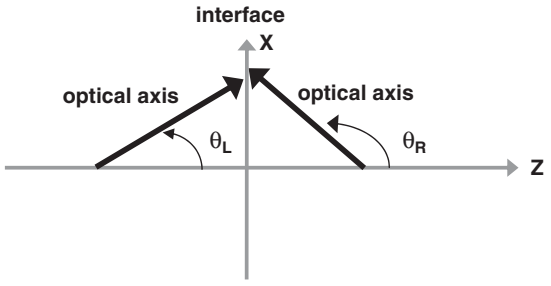

Fig. 1.2. The interface (the x–y plane) of two uniaxial anisotropic media

but isotropic permeabilities μ_{L} and μ_{R}, where L and R denote the left-hand and right-hand side, respectively. Their symmetry axes are assumed to lie in the same plane as the plane of incidence, which is also perpendicular to the interface, but nevertheless may incline at any angles with respect to the interface normal. In the principal coordinate system (x', y', z'), the relative permittivity tensors are given by

$$\varepsilon_{\mathrm{L,R}} = \begin{pmatrix} \varepsilon_1^{\mathrm{L,R}} & 0 & 0 \\ 0 & \varepsilon_1^{\mathrm{L,R}} & 0 \\ 0 & 0 & \varepsilon_3^{\mathrm{L,R}} \end{pmatrix}, \tag{1.3}$$

where ε_1 and ε_3 denote the dielectric components for electric field **E** polarized perpendicular and parallel to the symmetric axis. In the (x,y,z) coordinate system shown in Fig. 1.2, the tensor becomes

$$\varepsilon_{\mathrm{L,R}} = \begin{pmatrix} \varepsilon_1^{\mathrm{L,R}} \cos^2(\theta_{\mathrm{L,R}}) + \varepsilon_3^{\mathrm{L,R}} \sin^2(\theta_{\mathrm{L,R}}) & 0 & (\varepsilon_3^{\mathrm{L,R}} - \varepsilon_1^{\mathrm{L,R}}) \sin(\theta_{\mathrm{L,R}}) \cos(\theta_{\mathrm{L,R}}) \\ 0 & \varepsilon_1^{\mathrm{L,R}} & 0 \\ (\varepsilon_3^{\mathrm{L,R}} - \varepsilon_1^{\mathrm{L,R}}) \sin(\theta_{\mathrm{L,R}}) \cos(\theta_{\mathrm{L,R}}) & 0 & \varepsilon_3^{\mathrm{L,R}} \cos^2(\theta_{\mathrm{L,R}}) + \varepsilon_1^{\mathrm{L,R}} \sin^2(\theta_{\mathrm{L,R}}) \end{pmatrix}. \tag{1.4}$$

Rather generalized discussions for the reflection–refraction problem associated with the interface defined in Fig. 1.2 have been given in the literature for the situation of ε_1 and ε_3 both being positive [37,38]. For an ordinary wave with electric field **E** polarized in the y-direction, i.e., perpendicular to the plane of incidence (a TE wave), the problem is equivalent to an isotropic case with different dielectric constants $\varepsilon_1^{\mathrm{L}}$ and $\varepsilon_1^{\mathrm{R}}$ for the left-hand and right-hand side. It is the reflection and refraction of the extraordinary or **H**-polarized wave, i.e., with **E** polarized in the x–z plane (a TM wave), that has generally been found to be more interesting. For the E- and H-polarized waves, the dispersion relations are given below for the two coordinate systems:

$$k_x'^2 + k_z'^2 = \frac{\omega^2}{c^2} \mu \varepsilon_1, \tag{1.5E}$$

$$\frac{k_x'^2}{\varepsilon_3} + \frac{k_z'^2}{\varepsilon_1} = \frac{\omega^2}{c^2} \mu, \tag{1.5H}$$

and

$$k_x^2 + k_z^2 = \frac{\omega^2}{c^2} \mu \varepsilon_1, \tag{1.6E}$$

$$\frac{(k_x \cos\theta_0 - k_z \sin\theta_0)^2}{\varepsilon_3} + \frac{(k_x \sin\theta_0 + k_z \cos\theta_0)^2}{\varepsilon_1} = \frac{\omega^2}{c^2} \mu, \tag{1.6H}$$

where θ_0 is the inclined angle of the uniaxis of the medium with respect to the z-axis. The lateral component k_x is required to be conserved across the

interface and the two solutions for k_z (of $\pm$) are found to be (with k in the unit of ω/c) the following:

$$k_z^{\pm} = \pm\sqrt{\mu\varepsilon_1 - k_x^2}, \tag{1.7E}$$

$$k_z^{\pm} = \frac{k_x\delta \pm 2\sqrt{\gamma(\beta\mu - k_x^2)}}{2\beta}, \tag{1.7H}$$

where $\gamma = \varepsilon_1\varepsilon_3$, $\beta = \varepsilon_1 \sin^2\theta_0 + \varepsilon_3 \cos^2\theta_0$, $\delta = \sin(2\theta_0)(\varepsilon_1 - \varepsilon_3)$. The Poynting vector $\mathbf{S} = \mathbf{E}^* \times \mathbf{H}$, corresponding to $k_z^{\pm}$, can be given as

$$S_x^{\pm} = |E_y|^2 \frac{k_x}{c\mu\mu_0}, \tag{1.8E}$$

$$S_x^{\pm} = |H_y|^2 \frac{2\gamma k_x \mp \delta\sqrt{\gamma(\beta\mu - k_x^2)}}{2c\varepsilon_0\beta\gamma}, \tag{1.8H}$$

and

$$S_z^{\pm} = \pm\,|E_y|^2 \frac{\sqrt{\mu\varepsilon_1 - k_x^2}}{c\mu\mu_0}, \tag{1.9E}$$

$$S_z^{\pm} = \pm\,|H_y|^2 \frac{\sqrt{\gamma(\beta\mu - k_x^2)}}{c\varepsilon_0\gamma}, \tag{1.9H}$$

where E_y and H_y are the y components of $\mathbf{E}$ and $\mathbf{H}$, respectively. If the incident beam is assumed to arrive from the left upon the interface (i.e., energy flows along the $+z$ direction), one should choose from (1.7) the solution that can give rise to a positive S_z. Note that (1.8) and (1.9) are valid for either side of the interface, and positive as well as negative ε_1, ε_3, and μ. With these equations, we can conveniently discuss the conditions for realizing negative refraction and zero reflection. Note that for the E-polarized wave, the sign of $\mathbf{k}\cdot\mathbf{S}$ is only determined by that of ε_1, since $\mathbf{k}\cdot\mathbf{S} = |E_y|^2\omega\varepsilon_0\varepsilon_1$; for the H-polarized wave, it is only determined by μ, since $\mathbf{k}\cdot\mathbf{S} = |H_y|^2\omega\mu_0\mu$.

Since S_z is always required to be positive, the condition to realize negative refraction is simply to request a sign change of S_x across the interface. For realizing zero reflection, if one can assure the positive component of S_z to be continuous across the interface, the reflection will automatically be eliminated. Therefore, one does not need to consider explicitly the reflection [32].

If both media are isotropic, i.e., $\varepsilon_1 = \varepsilon_3 = \varepsilon$, we have $S_x \propto k_x/\mu$ and $S_z^{\pm} \propto \pm\sqrt{\mu\varepsilon - k_x^2}/\mu$ for the E-polarized wave, $S_x \propto k_x/\varepsilon$ and $S_z^{\pm} \propto \pm\sqrt{\varepsilon^2(\varepsilon\mu - k_x^2)}/\varepsilon^2$ for the H-polarized wave. To have negative refraction for both of the polarizations, the only possibility is to have ε and μ changing sign simultaneously. To have zero reflection for any k_x, the conditions become $|\varepsilon^{\mathrm{L}}| = |\varepsilon^{\mathrm{R}}|$ and $|\mu^{\mathrm{L}}| = |\mu^{\mathrm{R}}|$, and $(\varepsilon\mu)^{\mathrm{L}} = (\varepsilon\mu)^{\mathrm{R}}$. Since $\varepsilon\mu > 0$ is necessary for the propagating wave, the conditions become $\varepsilon^{\mathrm{L}} = -\varepsilon^{\mathrm{R}}$ and $\mu^{\mathrm{L}} = -\mu^{\mathrm{R}}$, as derived by Veselago [10]. It is interesting to note that if one of the media is

replaced with a photonic crystal with a negative effective refractive index, the "impedance" matching conditions become much more restrictive. In has been found that to minimize the reflection the surrounding medium has to have a pair of specific ε and μ for a given photonic crystal [60] and the values could even depend on the surface termination of the photonic crystal [61].

If the media are allowed to be anisotropic, several ways exist to achieve negative refraction, even if we limit ourselves to μ being isotropic. For the E-polarized wave, since $S_x \propto k_x/\mu$, negative refraction requires $\mu < 0$ on one side, assuming $\mu^{\mathrm{R}} < 0$ (the left-hand side is assumed to have everything positive). In the meantime, because $S_z \propto \pm\sqrt{\mu\varepsilon_1 - k_x^2}/\mu$, one also needs to have $\varepsilon_1^{\mathrm{R}} < 0$ to make the wave propagative. Thus, with $\varepsilon_1^{\mathrm{R}} < 0$ and $\mu^{\mathrm{R}} < 0$ while keeping $\varepsilon_3^{\mathrm{R}} > 0$, one can have negative refraction, and zero reflection for the E-polarized wave occurring for any k_x when $\mu^{\mathrm{R}} = -\mu^{\mathrm{L}}$ and $(\varepsilon_1\mu)^{\mathrm{L}} = (\varepsilon_1\mu)^{\mathrm{R}}$. This situation is similar to the isotropic case with $\varepsilon = \varepsilon_1$, although there will be no negative refraction for the H-polarized wave.

For the H-polarized wave, if both media are allowed to be anisotropic but the symmetry axes are required to be normal to the interface (i.e., $\theta_{\mathrm{L}} = \theta_{\mathrm{R}} = 0°$), we have $S_x \propto k_x/\varepsilon_3$ and $S_z \propto \pm\sqrt{\varepsilon_1\varepsilon_3(\varepsilon_3\mu - k_x^2)}/(\varepsilon_1\varepsilon_3) > 0$. Negative refraction requires $\varepsilon_3 < 0$ on one side, again assumed to be the right-hand side (the left-hand side is assumed to have everything positive). If $\varepsilon_1 < 0$, then $\mu^{\mathrm{R}} < 0$ is also needed to have a propagating wave; we have $S_z^R \propto \sqrt{\varepsilon_1^{\mathrm{R}}\varepsilon_3^{\mathrm{R}}(\varepsilon_3^{\mathrm{R}}\mu^{\mathrm{R}} - k_x^2)}/(\varepsilon_1^{\mathrm{R}}\varepsilon_3^{\mathrm{R}})$, and the conditions for zero reflection are $(\varepsilon_1\varepsilon_3)^{\mathrm{L}} = (\varepsilon_1\varepsilon_3)^{\mathrm{R}}$ and $(\varepsilon_3\mu)^{\mathrm{L}} = (\varepsilon_3\mu)^{\mathrm{R}}$. If $\varepsilon_1^{\mathrm{R}} > 0$, then $\mu^{\mathrm{R}} > 0$ is necessary to have a propagating wave; we have $S_z^{\mathrm{R}} \propto -\sqrt{\varepsilon_1^{\mathrm{R}}\varepsilon_3^{\mathrm{R}}(\varepsilon_3^{\mathrm{R}}\mu^{\mathrm{R}} - k_x^2)}/(\varepsilon_1^{\mathrm{R}}\varepsilon_3^{\mathrm{R}})$, but zero reflection is not possible except for $k_x = 0$ and when $(\varepsilon_1\varepsilon_3)^{\mathrm{L}} = |\varepsilon_1\varepsilon_3|^{\mathrm{R}}$ and $|\varepsilon_3\mu|^{\mathrm{L}} = |\varepsilon_3\mu|^{\mathrm{R}}$. The results for $\theta_{\mathrm{L}} = \theta_{\mathrm{R}} = 90°$ can be obtained by simply replacing ε_3 with ε_1 in the results for $\theta_{\mathrm{L}} = \theta_{\mathrm{R}} = 0°$. Similar or somewhat different cases have been discussed in the literature for either $\theta_{\mathrm{L}} = \theta_{\mathrm{R}} = 0°$ or $\theta_{\mathrm{L}} = \theta_{\mathrm{R}} = 90°$, leading to the conclusion that at least one component of either ε or $\boldsymbol{\mu}$ tensor needs to be negative to realize negative refraction [62–66].

However, the relaxation on the restriction of the optical axis orientations, allowing $0 < \theta_{\mathrm{L}} < 90°$ and $0 < \theta_{\mathrm{R}} < 90°$, makes negative refraction and zero reflection possible even if both ε and $\boldsymbol{\mu}$ tensors are positive definite. When ε is positive definite, we have $\gamma > 0$ and $\beta > 0$, and in this case $\mu > 0$ is necessary to have propagating modes. The condition for zero reflection can be readily found to be $\gamma^{\mathrm{L}} = \gamma^{\mathrm{R}}$, and $(\beta\mu)^{\mathrm{L}} = (\beta\mu)^{\mathrm{R}}$. For the case of the interface being that of a pair of twinned crystals [31], these requirements are automatically satisfied for any angle of incidence. The twinned structure assures that the zero-reflection condition is valid for any wavelength, despite the existence of dispersion; however, for the more-general case using two different materials, the condition can at best be satisfied at discrete wavelengths because the dispersion effect may break the matching condition, similar to the case of $\varepsilon = \mu = -1$. The negative-refraction condition can be derived from (1.8H) (since $\gamma > 0$, S_x^+ should be used). Note that $S_x^+ = 0$ at $k_{x0} = \delta\sqrt{\beta\mu}/\sqrt{4\gamma + \delta^2}$. If $k_{x0}^{\mathrm{L}} < k_{x0}^{\mathrm{R}} (k_{x0}^{\mathrm{L}} > k_{x0}^{\mathrm{R}})$, S_x changes sign across the interface or negative

refraction occurs in the region $k_{x0}^{\mathrm{L}} < k_x < k_{x0}^{\mathrm{R}} (k_{x0}^{\mathrm{R}} < k_x < k_{x0}^{\mathrm{L}})$. For the crystal twin with $\theta_{\mathrm{L}} = \pi/4$ and $\theta_{\mathrm{R}} = -\pi/4$, $k_{x0}^{\mathrm{L}} = -k_{x0}^{\mathrm{R}} = (\varepsilon_1 - \varepsilon_3)/\sqrt{2(\varepsilon_1 + \varepsilon_3)})$. When $\varepsilon_3 > \varepsilon_1$ (i.e., positive birefringence) in the region of $k_{x0}^{\mathrm{L}} < k_x < k_{x0}^{\mathrm{R}}$, $S_x^{\mathrm{L}} > 0$ and $S_x^{\mathrm{R}} < 0$. For any given θ_{L}, ε_1, and ε_3, the maximum bending of the light beam or the strongest negative refraction occurs when $k_x = 0$ and $\sin^2 \theta_{\mathrm{L}} = \varepsilon_3/(\varepsilon_1 + \varepsilon_3)$, where the propagation direction of the light is given by $\phi = \arctan(S_x/S_z) = \arctan[-\delta/(2\beta)]$ for each side, and the amount of bending is measured by $\phi_{\mathrm{L}} - \phi_{\mathrm{R}} = 2\arctan[-\delta_{\mathrm{L}}/(2\beta)]$. For any given θ_{L} (as defined in Fig. 1.2), the maximum amount of bending is $2\theta_{\mathrm{L}}$ for positive crystal ($\varepsilon_3 > \varepsilon_1$ and $0 < \theta_{\mathrm{L}} < \pi/2$) or $2(\theta_{\mathrm{L}} - \pi/2)$ for negative crystal ($\varepsilon_1 > \varepsilon_3$ and $\pi/2 < \theta_{\mathrm{L}} < \pi$), when either $\varepsilon_1/\varepsilon_3 \to \infty$ or $\varepsilon_3/\varepsilon_1 \to \infty$. Figure 1.3 shows an experimental demonstration of amphoteric refraction with minimal reflection loss realized with a YVO_4 bicrystal [31], and Fig. 1.4 compares the experimental and theoretical results for the relationship between the angles of incidence and refraction (note that $\theta_{\mathrm{L}} = -\pi/4$ and $\theta_{\mathrm{R}} = \pi/4$ are assumed) [31].

As a special case of the general discussion with $0 < \theta_{\mathrm{L}} < 90^\circ$ and $0 < \theta_{\mathrm{R}} < 90^\circ$, zero reflection and/or negative refraction can also be realized at an isotropic–anisotropic interface [32–36]. Assuming $\mu = 1$, zero reflection occurs when $\varepsilon^{\mathrm{L}} = \sqrt{\varepsilon_1{}^{\mathrm{R}} \varepsilon_3{}^{\mathrm{R}}}$, which actually is the condition for the so-called perfectly matched layer [67]. The interface of air and a uniaxial crystal with

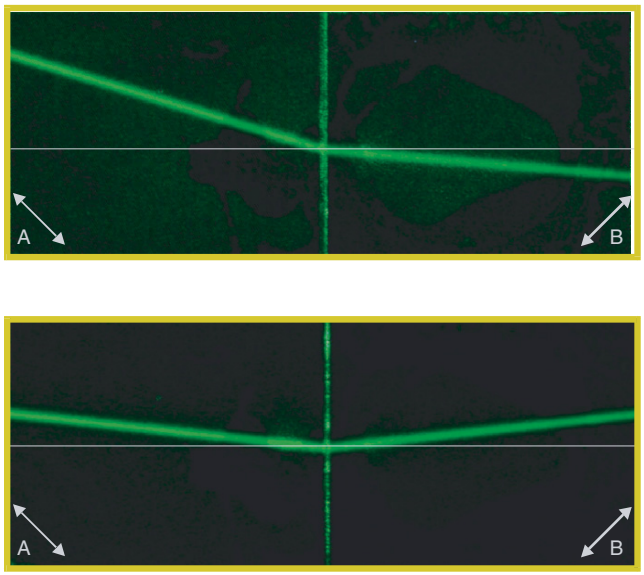

Fig. 1.3. Images of light propagation in a YVO_4 bicrystal. The *upper panel* shows an example of normal (positive) refraction, whereas the *lower panel* shows abnormal (negative) refraction. Note that no reflection at the bicrystal interface is visible to the naked eye. The interface is illuminated by inadvertently scattered light. The *arrows* indicate the orientations of the optical axes (A – *left*, B – *right*)

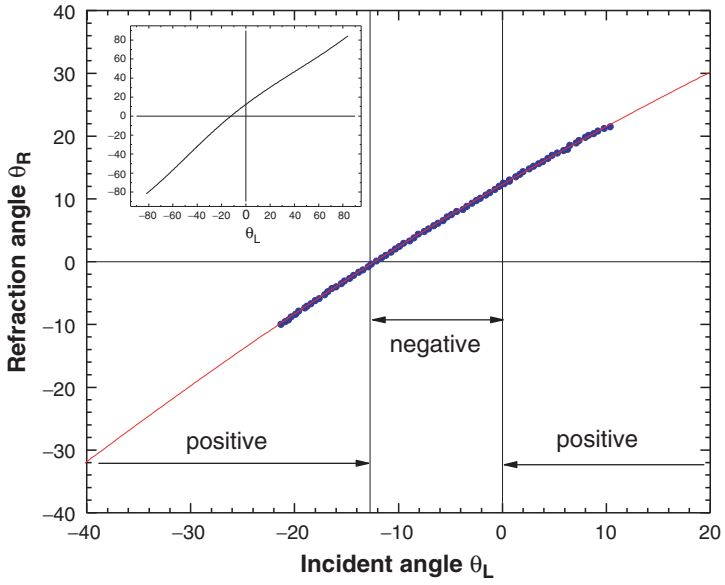

Fig. 1.4. Comparison of theoretical predictions with experimental data. Amphoteric refraction in a YVO_4 bicrystal is divided into three regions: one negative ($\theta_R/\theta_L < 0$) and two positive ($\theta_R/\theta_L > 0$). The data points are measured with a 532-nm laser light, and the curve is calculated with the refractive index of the material ($n_o = 2.01768$ and $n_e = 2.25081$). Inset: the full operation range of the device

its optical axis oriented at a nonzero angle to the interface normal is perhaps the simplest interface to facilitate negative refraction, as illustrated in Fig. 1.1. However trivial it might be, it is a genuine phenomenon of negative refraction.

If $\mu^R < 0$ and the ε^R tensor is indefinite or not positive definite, while allowing $0 < \theta_L < 90°$ and $0 < \theta_R < 90°$, we will have more unusual situations of refraction. Again, all parameters on the left-hand side are assumed positive, and, for simplicity, the left medium is assumed to be isotropic. If both $\varepsilon_1^R < 0$ and $\varepsilon_3^R < 0$, then the results are qualitatively similar to that of the isotropic case discussed above. However, when $\varepsilon_1^R < 0$ but $\varepsilon_3^R > 0$, or when ${\varepsilon_1}^R > 0$ but $\varepsilon_3^R < 0$, we thus have $\gamma^R < 0$; and by appropriately choosing θ_R to have $\beta^R > 0$, we have $\sqrt{\gamma^R(\beta^R\mu^R - k_x^2)} = \sqrt{|\gamma^R|\,(\beta^R\,|\mu^R| + k_x^2)}$, which indicates that all the real k_x components are propagating modes, and therefore, there will be no evanescent wave. For these cases, $(S_z^-)^R > 0$, and it is always possible to choose a value of θ_R (e.g., $\theta_R = 45°$ when ${\varepsilon_3}^R > |\varepsilon_1^R|$ or $\theta_R = -45°$ when ${\varepsilon_1}^R > |\varepsilon_3^R|$) such that $\delta^R < 0$; and thus, $(S_x^-)^R > 0$ for any k_x, which means that there will be no negative refraction for $k_x > 0$, in spite of the medium being left handed (because of $\mu^R < 0$), although refraction is negative for $k_x < 0$. Zero reflection only occurs at $k_x = 0$, when $\varepsilon^L = \sqrt{|\varepsilon_1^R \varepsilon_3^R|}$ and $(\varepsilon\mu)^L = |\beta\mu|^R$.

In summary, having an LHM is neither a necessary nor a sufficient condition for achieving negative refraction. The left-handed behavior does not always lead to evanescent wave amplification. It may not always be possible to match the material parameters to eliminate the interface reflection with an LHM. The double-negativity lens proposed by Veselago and Pendry represents the most-stringent material requirement to achieve negative refraction, zero reflection, and evanescent wave amplification. For a uniform medium, the left-handed behavior can only be obtained with at least one component of the ε or μ tensor being negative: ε_1 for the **E**-polarized wave and μ_1 for the **H**-polarized wave, if limited to materials with uniaxial symmetry [63]. However, once one of the components of either the ε or μ tensor becomes negative so as to have left-handed behavior, then at least one of the components of the other tensor needs to be negative to have propagating modes in the medium, and possibly to have evanescent wave amplification (as discussed above for the **H**-polarized wave and in the literature for the **E**-polarized wave [65]).

Analogous to the discussion of negative refraction in the photonic crystal, one could consider the propagation of a ballistic electron beam in a real crystal. It is perceivable that one could discuss how various types of electronic band structures might bend the electron beam negatively, in a manner similar to the negative "refraction" discussions for the photonic crystal [40]. Again, a domain twin interface, as the one shown in Fig. 1.5 for example, appears to be a simple case that can give rise to negative refraction and zero reflection for a ballistic electron beam [31]. It is a genuine refraction when light goes through such an interface; but for the electron beam, it is fundamentally a phenomenon of diffraction. Complex structures of this type of domain twin could be of great interest for both optics and electronics. Examples of such super structures created by stacking domain twins in a linear manner

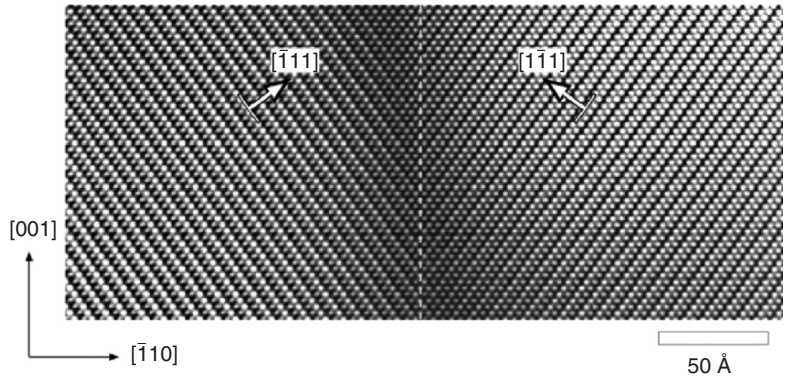

Fig. 1.5. A typical high-resolution cross-sectional transmission electron microscopy (TEM) image of domain twin structures frequently observed in CuPt-ordered III–V semiconductor alloys (e.g., GaInAs). The ordering directions are [$\bar{1}$11] (*left*) and [1$\bar{1}$1] (*right*). The *vertical dashed line* indicates the twin boundary

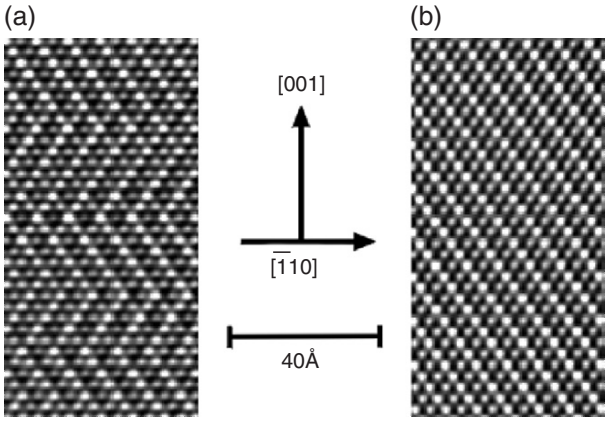

Fig. 1.6. High-resolution cross-sectional TEM images of ordered GaInP alloys: (**a**) double-variant ordered structure with quasiperiodic stacking of domain twins along the [001] direction, and (**b**) single-variant ordered domain

can be found in the literature, though not in the context of negative refraction. For instance, a zig-zag structure found in the so-called "sculptured" thin film is ideally a periodic one-dimensional stacking of the domain twins. Zero reflection for the TM polarized electromagnetic wave was indicated in the literature (for normal incidence [68] and arbitrary angle of incidence [69]). For electronics, an unusual type of semiconductor superlattice, termed an "orientational superlattice," was found in spontaneously ordered semiconductor alloys, and their electronic structures and optical properties were also investigated [70–72]. Figure 1.6 shows a quasiperiodic structure of ordered domain twins, which is an orientational superlattice, in a $Ga_{1-x}In_xP$ alloy [72].

1.3 Conclusion

Negative refraction, as an interesting physical phenomenon, can be observed in a number of circumstances possibly facilitated by very different physical mechanisms. The interest in this field has provided great opportunities for fundamental physics research, material developments, and novel applications.

Acknowledgments

We thank Drs. V.M. Agranovich, C.M. Krowne, B. Fluegel, and S. Smith for helpful discussions. This work was funded by the US Department of Energy, Office of Science, Basic Energy Sciences, under Contract No. DE-AC36-99GO10337 to NREL.

References

1. J.B. Pendry, Phys. Rev. Lett. **85**, 3966 (2000)
2. J.B. Pendry, Science **305**, 788 (2005)
3. J.B. Pendry, D.R. Smith, Phys. Today **57**, 37 (2004)
4. Y. Zhang, A. Mascarenhas, Mod. Phys. Lett. B **18** (2005)
5. A. Schuster, *An Introduction to the Theory of Optics* (Edward Arnold, London, 1904)
6. E.I. Rashba, J. Appl. Phys. **79**, 4306 (1996)
7. C.F. Klingshirn, *Semiconductor Optics* (Springer, Berlin Heidelberg New York, 1995)
8. G. Dolling, C. Enkrich, M. Wegener, C.M. Soukoulis, S. Linden, Science **312**, 892 (2006)
9. V.M. Agranovich, V. L. Ginzburg, *Spatial Dispersion in Crystal Optics and the Theory of Excitons* (Wiley, London, 1966)
10. V.G. Veselago, Sov. Phys. Usp. **10**, 509 (1968)
11. A.I. Viktorov, *Physical Principles of the Use of Ultrasonic Raleigh and Lamb Waves in Engineering* (Nauka, Russia, 1966)
12. P.V. Burlii, I.Y. Kucherov, JETP Lett. **26**, 490 (1977)
13. H. Lamb, Proc. London Math. Soc. Sec. II **1**, 473 (1904)
14. C.M. Krowne, *Encyclopedia of Rf and Microwave Engineering*, vol. 3 (Wiley, New York, 2005), p. 2303
15. M. Born, E. Wolf, *Principles of Optics* (Cambridge University Press, Cambridge, 1999)
16. J. Neufeld, R.H. Ritchie, Phys. Rev. **98**, 1955 (1955)
17. V.L. Ginzburg, JETP **34**, 1096 (1958)
18. V.M. Agranovich, Y.R. Shen, R.H. Baughman, A.A. Zakhidov, Phys. Rev. B **69**, 165112 (2004)
19. M. Born, K. Huang, *Dynamical Theory of Crystal Lattices* (Clarendon, Oxford, 1954)
20. J.J. Hopfield, Phys. Rev. **112**, 1555 (1958)
21. V.M. Agranovich, Y.R. Shen, R.H. Baughman, A.A. Zakhidov, J. Lumin. **110**, 167 (2004)
22. V.E. Pafomov, Sov. Phys. JETP **36**, 1321 (1959)
23. R.A. Shelby, D.R. Smith, S. Schultz, Science **292**, 77 (2001)
24. L.D. Landau, E.M. Lifshitz, L.P. Pitaevskii, *Electrodynamics of Continuous Media* (Butterworth-Heinemann, Oxford, 1984)
25. C. Enkrich, M. Wegener, S. Linden, S. Burger, L. Zschiedrich, F. Schmidt, J.F. Zhou, T. Koschny, C.M. Soukoulis, Phys. Rev. Lett. **95** (2005)
26. A.N. Grigorenko, A.K. Geim, H.F. Gleeson, Y. Zhang, A.A. Firsov, I.Y. Khrushchev, J. Petrovic, Nature **438**, 335 (2005)
27. S. Zhang, W.J. Fan, N.C. Panoiu, K.J. Malloy, R.M. Osgood, S.R.J. Brueck, Phys. Rev. Lett. **95** (2005)
28. S. Linden, C. Enkrich, M. Wegener, J.F. Zhou, T. Koschny, C.M. Soukoulis, Science **306**, 1351 (2004)
29. V.M. Shalaev, W.S. Cai, U.K. Chettiar, H.K. Yuan, A.K. Sarychev, V.P. Drachev, A.V. Kildishev, Opt. Lett. **30**, 3356 (2005)
30. J.B. Pendry, Science **306**, 1353 (2004)
31. Y. Zhang, B. Fluegel, A. Mascarenhas, Phys. Rev. Lett. **91**, 157404 (2003)
32. Y. Zhang, A. Mascarenhas, in *Mat. Res. Soc. Symp. Proc.*, vol. 794 (MRS Fall Meeting, Boston, 2003), p. T10.1

33. L.I. Perez, M.T. Garea, R.M. Echarri, Opt. Commun. **254**, 10 (2005)
34. X.L. Chen, H. Ming, D. YinXiao, W.Y. Wang, D.F. Zhang, Phys. Rev. B **72**, 113111 (2005)
35. Y.X. Du, M. He, X.L. Chen, W.Y. Wang, D.F. Zhang, Phys. Rev. B **73**, 245110 (2006)
36. Y. Lu, P. Wang, P. Yao, J. Xie, H. Ming, Opt. Commun. **246**, 429 (2005)
37. Z. Liu, Z.F. Lin, S.T. Chui, Phys. Rev. B **69**, 115402 (2004)
38. Y. Wang, X.J. Zha, J.K. Yan, Europhys. Lett. **72**, 830 (2005)
39. K. Sakoda, *Optical Properties of Photonic Crystals* (Springer, Berlin Heidelberg New York, 2001)
40. S. Foteinopoulou, C.M. Soukoulis, Phys. Rev. B **72**, 165112 (2005)
41. M. Notomi, Phys. Rev. B **62**, 10696 (2000)
42. P.V. Parimi, W.T.T. Lu, P. Vodo, S. Sridhar, Nature **426**, 404 (2003)
43. C. Luo, S.G. Johnson, J.D. Joannopoulos, J.B. Pendry, Phys. Rev. B **65**, 201104 (2002)
44. E. Cubukcu, K. Aydin, E. Ozbay, S. Foteinopoulou, C.M. Soukoulis, Nature **423**, 604 (2003)
45. A.B. Pippard, *The Dynamics of Conduction Electrons* (Gordon and Breach, New York, 1965)
46. Y.R. Shen, *The Principles of Nonlinear Optics* (Wiley, New York, 1984)
47. L. Silvestri, O.A. Dubovski, G.C. La Rocca, F. Bassani, V.M. Agranovich, Nuovo Cimento Della Societa Italiana Di Fisica C-Geophysics and Space Physics **27**, 437 (2004)
48. C. Luo, S.G. Johnson, J.D. Joannopoulos, J.B. Pendry, Phys. Rev. B **68**, 45115 (2003)
49. A.L. Pokrovsky and A.L. Efros, Phys. B **338**, 333 (2003)
50. D.R. Smith, D. Schurig, M. Rosenbluth, S. Schultz, S.A. Ramakrishna, J.B. Pendry, Appl. Phys. Lett. **82**, 1506 (2003)
51. I. Ichimura, S. Hayashi, G.S. Kino, Appl. Opt. **36**, 4339 (1997)
52. http://www.semiconductor-technology.com/features/section290/
53. S.M. Mansfield, G.S. Kino, Appl. Phys. Lett. **57**, 2615 (1990)
54. I. Smolyaninov, J. Elliott, A.V. Zayats, C.C. Davis, Phys. Rev. Lett. **94** (2005)
55. Z.F. Feng, X.D. Zhang, Y.Q. Wang, Z.Y. Li, B.Y. Cheng, D.Z. Zhang, Phys. Rev. Lett. **94** (2005)
56. Z. Lu, J.A. Murakowski, C.A. Schuetz, S. Shi, G.J. Schneider, D.W. Prather, Phys. Rev. Lett. **95**, 153901 (2005)
57. N. Fang, H. Lee, C. Sun, X. Zhang, Science **308**, 534 (2005)
58. D.O.S. Melville, R.J. Blaikie, Opt. Express **13**, 2127 (2005)
59. J.M. Vigoureux, D. Courjon, Appl. Opt. **31**, 3170 (1992)
60. A.L. Efros, A.L. Pokrovsky, Solid State Commun. **129**, 643 (2004)
61. T. Decoopman, G. Tayeb, S. Enoch, D. Maystre, B. Gralak, Phys. Rev. Lett. **97** (2006)
62. I.V. Lindell, S.A. Tretyakov, K.I. Nikoskinen, S. Ilvonen, Microw. Opt. Technol. Lett. **31**, 129 (2001)
63. L.B. Hu, S.T. Chui, Phys. Rev. B **66**, 085108 (2002)
64. L. Zhou, C.T. Chan, P. Sheng, Phys. Rev. B **68**, 115424 (2003)
65. D.R. Smith, D. Schurig, Phys. Rev. Lett. **90**, 077405 (2003)
66. T. Dumelow, J.A.P. da Costa, V.N. Freire, Phys. Rev. B **72** (2005)
67. S.D. Gedney, IEEE Trans. Antennas Propagat. **44**, 1630 (1996)

68. A. Lakhtakia, R. Messier, Opt. Eng. **33**, 2529 (1994)
69. G.Y. Slepyan, A.S. Maksimenko, Opt. Eng. **37**, 2843 (1998)
70. Y. Zhang, A. Mascarenhas, Phys. Rev. B **55**, 13100 (1997)
71. Y. Zhang, A. Mascarenhas, S.P. Ahrenkiel, D.J. Friedman, J. Geisz, J.M. Olson, Solid State Commun. **109**, 99 (1999)
72. Y. Zhang, B. Fluegel, S.P. Ahrenkiel, D.J. Friedman, J. Geisz, J.M. Olson, A. Mascarenhas, Mat. Res. Soc. Symp. Proc. **583**, 255 (2000)

2

Anisotropic Field Distributions in Left-Handed Guided Wave Electronic Structures and Negative Refractive Bicrystal Heterostructures

C.M. Krowne

Summary. Effect of anisotropy in the physical tensor description of the negative index of refraction material acting as a substrate is found on the electromagnetic field distributions. This is done for the case of a microstrip structure whose configuration is commonly used in microwave and millimeter wave integrated circuits. These ab initio studies have been done self-consistently with a computer code using a full-wave integral equation numerical method based upon a generalized anisotropic Green's function utilizing appropriate boundary conditions. Field distributions are provided over two decades of frequency in the cross-section of the uniform guided wave structure, from 0.2 to 20 GHz. It is found that modifying the tensor can allow control because the wave changes volumetrically, or switches from volumetric to surface, in its distribution of fields. It has also been discovered that heterostructure bicrystal arrangements lead to field asymmetry in guided wave structures. A study is conducted over a range of nominal permittivity values to see if the effect is present in widely varying dielectric materials. Marked shifts of the field distribution occurs in some cases, and this can be the basis of an all electronic device that provides beam steering or a device that gives directional action. Such all electronic devices could be fixed or even constructed as control components using materials with electrostatically controllable permittivity. Distributions have been obtained to demonstrate the effect using an anisotropic Green's function solver.

2.1 Anisotropic Field Distributions in Left-Handed Guided Wave Electronic Structures

2.1.1 Introduction

Although considerable physics has been learned about the dispersion behavior and electromagnetic fields for propagation down guided wave microstrip structures loaded with DNM (double-negative materials with simultaneous negative permittivity and permeability) which are also referred to LHM (left-handed materials for the left-handed orientation of the electric, magnetic, and propagation phase constant) [1, 2] nothing is known about what happens to

the field distributions as anisotropy is introduced. This is an extremely interesting area since maintenance of isotropy has been recognized to be essential for 3D imaging possibilities [3, 4], and such isotropy should also be necessary for arbitrary field contouring or arrangement of fields in small electronic devices which are created especially to employ the unique properties of DNM. It should also be noted here that these materials can be referred to as NIRM (negative index of refraction materials) or NIM (negative index materials). Furthermore, because the essential property of these materials is opposite orientations of the phase velocity and the Poynting vector (giving the power flow direction), they may be referred to as alternatively as negative phase velocity materials (NPV materials or simply NPVM) [5].

Because we are not going to further examine 3D imaging issues, but 3D behavior of fields in electronic devices, we will restrict the use of notation when referring to these materials as DNM or NPVM. Although maintaining isotropy for many integrated circuit applications may be desirable as mentioned above, it may also be desirable to introduce anisotropy [6, 7], or at least find it acceptable to have some anisotropy in certain device configurations, where because of the particular applications, the effective dimensions of the device is reduced from 3D to 2D or even 1D. This is not some idle speculation, as quasilumped element realizations using distributed and/or lumped sections have been used to make components employing backward wave behavior, one of the hallmarks of DNM or NPVM [8–11]. Thus, whether or not we want to examine what the effect is of some deviation from isotropy, or wish to intentionally introduce anisotropy, it would be very instructive to undertake such an investigation.

In pursuing this quest, the backdrop of already studied field distributions for isotropic DNM in the C-band, X-band, Ka and V-bands, and W-band broadcast frequency regions gives us some basis upon which to begin these studies. In the C-band region, electromagnetic field line plots of $\mathbf{E}_\mathrm{t}$ and $\mathbf{H}_\mathrm{t}$ for the transverse fields in the cross-section perpendicular to the propagation direction were provided at 5 GHz [2]. Also given were simultaneous magnitude and arrow vector distributions plots for $E/\mathbf{E}_\mathrm{t}$ and $H/\mathbf{H}_\mathrm{t}$ at the same frequency. Finally, a Poynting vector distribution plot P_z was provided at 5 GHz. In the X-band region, electromagnetic field line plots of $\mathbf{E}_\mathrm{t}$ and $\mathbf{H}_\mathrm{t}$ were provided at 10 GHz [12]. Also given were simultaneous magnitude and arrow vector distributions plots for $E/\mathbf{E}_\mathrm{t}$ and $H/\mathbf{H}_\mathrm{t}$ at the same frequency. Finally, a Poynting vector distribution plot P_z was provided at 10 GHz. In the overlap region between the Ka and V-bands, electromagnetic field plots of simultaneous magnitude and arrow vector distributions plots for $E/\mathbf{E}_\mathrm{t}$ and $H/\mathbf{H}_\mathrm{t}$ were given at 40 GHz [12, 13]. Simultaneous line and magnitude distribution plots for $E/\mathbf{E}_\mathrm{t}$ and $H/\mathbf{H}_\mathrm{t}$ were also provided at 40 GHz [12]. Lastly, a Poynting vector distribution plot P_z was provided at the same frequency [12].

Sections 2.1.2 and 2.1.3 cover, respectively, the governing equations/acquisition of the anisotropic Green's function, and use of basis current functions/determination of the propagation constant and electromagnetic

fields, for the guided wave microstrip structure with anisotropic DNM. With a complete development in hand, numerical calculations are performed in Sect. 2.1.4 for a microstrip structure at three frequencies offset from each other by decade steps. Each study is begun by first examining an isotropic tensor to provide a reference standard for looking at the effects of introducing anisotropy through a permittivity tensor. Once the electromagnetic distributions have been obtained for the isotropic case, distributions for anisotropy are calculated. This process of first finding the isotropic result, then proceeding on to the anisotropic situation, is done at each frequency.

2.1.2 Anisotropic Green's Function Based Upon LHM or DNM Properties

Maxwell's time varying equations describe the electromagnetic field behavior in a medium if they are combined with constitutive relationships embedding the physical properties of the medium in them. Maxwell's two curl equations are

$$\nabla \times \mathbf{E}(t,\mathbf{x}) = -\frac{\partial \mathbf{B}(t,\mathbf{x})}{\partial t}, \quad \nabla \times \mathbf{H}(t,\mathbf{x}) = \frac{\partial \mathbf{D}(t,\mathbf{x})}{\partial t} + \mathbf{J}(t,\mathbf{x}). \tag{2.1}$$

Constitutive relationships are

$$\mathbf{D}(t,\mathbf{x}) = \bar{\bar{\varepsilon}}\mathbf{E}(t,\mathbf{x}) + \bar{\bar{\rho}}\mathbf{H}(t,\mathbf{x}), \quad \mathbf{B}(t,\mathbf{x}) = \bar{\bar{\rho}}'\mathbf{E}(t,\mathbf{x}) + \bar{\bar{\mu}}\mathbf{H}(t,\mathbf{x}). \tag{2.2}$$

Here $\mathbf{x} = (\mathrm{x}_1, \mathrm{x}_2, \mathrm{x}_3) = (\mathrm{x}, \mathrm{y}, \mathrm{z})$. Most general NPV medium can have all constitutive tensors in (2.2) nonzero, including the magnetoelectric or optical activity tensors $\bar{\bar{\rho}}$ and $\bar{\bar{\rho}}'$, as they are sometimes called. The formulation is therefore kept general in order to retain the most flexibility for studying materials with widely varying physical properties. Because many problems are often transparent in the frequency domain, and because nonharmonic problems can be resolved into a superposition of time-harmonic components, we elect to study here time harmonic electromagnetic wave propagation through the solid state LHM–RHM structure (RHM, right-handed medium or ordinary medium). Taking the time harmonic variation to be of a form $\mathrm{e}^{\mathrm{i}\omega t}$, Maxwell's equation become

$$\nabla \times \mathbf{E}(\mathbf{x}) = -\mathrm{i}\omega\mathbf{B}(\mathbf{x}), \quad \nabla \times \mathbf{H}(\mathbf{x}) = \mathrm{i}\omega\mathbf{D}(\mathbf{x}) + \mathbf{J}(\mathbf{x}) \tag{2.3}$$

with the constitutive relationships dropping the explicit t-dependence

$$\mathbf{D}(\mathbf{x}) = \bar{\bar{\varepsilon}}(\omega)\mathbf{E}(\mathbf{x}) + \bar{\bar{\rho}}(\omega)\mathbf{H}(\mathbf{x}), \quad \mathbf{B}(\mathbf{x}) = \bar{\bar{\rho}}'(\omega)\mathbf{E}(\mathbf{x}) + \bar{\bar{\mu}}(\omega)\mathbf{H}(\mathbf{x}). \tag{2.4}$$

Dependence of the constitutive parameters on radian frequency is a well-recognized fact and that is why explicit variation on $\boldsymbol{\omega}$ is shown. However, for the study to be conducted here at specific frequencies, we do not need to call

out this dependence explicitly. We will be setting for, example $\bar{\bar{\varepsilon}}(\omega) = v$ for $\omega = \omega_v$. Therefore, we set

$$\mathbf{D}(\mathbf{x}) = \bar{\bar{\varepsilon}}\mathbf{E}(\mathbf{x}) + \bar{\bar{\rho}}\mathbf{H}(\mathbf{x}), \quad \mathbf{B}(\mathbf{x}) = \bar{\bar{\rho}}'\mathbf{E}(\mathbf{x}) + \bar{\bar{\mu}}\mathbf{H}(\mathbf{x}) \tag{2.5}$$

and understand it means (2.2).

Curl equations (2.1) may be combined into a single sourceless governing equation [14],

$$L_{\mathrm{T}}(\mathbf{x})\mathbf{V}_{\mathrm{L}}(\mathbf{x}) = \mathrm{i}\omega\mathbf{V}_{\mathrm{R}}(\mathbf{x}), \tag{2.6}$$

where the matrix partial differential operator acting on the **E**–**H** column vector is

$$L_{\mathrm{T}}(\mathbf{x}) = \begin{bmatrix} 0 & L_{\mathrm{q}}(\mathbf{x}) \\ -L_{\mathrm{q}}(\mathbf{x}) & 0 \end{bmatrix}, \tag{2.7}$$

where the quadrant operator is

$$L_{\mathrm{q}}(\mathbf{x}) = \begin{bmatrix} 0 & -\dfrac{\partial}{\partial z} & \dfrac{\partial}{\partial y} \\ \dfrac{\partial}{\partial z} & 0 & -\dfrac{\partial}{\partial x} \\ -\dfrac{\partial}{\partial y} & \dfrac{\partial}{\partial x} & 0 \end{bmatrix}. \tag{2.8}$$

Current **J** effects are introduced later through a Green's function process [see (2.80)]. Vectors in (2.6) are

$$\mathbf{V}_{\mathrm{L}}(\mathbf{x}) = \begin{bmatrix} E_x \\ E_y \\ E_z \\ H_x \\ H_y \\ H_z \end{bmatrix} = \begin{bmatrix} \mathbf{E} \\ \mathbf{H} \end{bmatrix}, \quad \mathbf{V}_{\mathrm{R}}(\mathbf{x}) = \begin{bmatrix} D_x \\ D_y \\ D_z \\ B_x \\ B_y \\ B_z \end{bmatrix} = \begin{bmatrix} \mathbf{D} \\ \mathbf{B} \end{bmatrix}. \tag{2.9}$$

Restricting ourselves to a guided wave structure with the wave traveling in a uniform cross-section in the z-direction, that is the wave has the form $\mathrm{e}^{\mathrm{i}\omega t - \gamma z}$, $\gamma = \gamma(\omega)$, simplifies (2.6)–(2.8) to

$$L_{\mathrm{T}}(x,y)\mathbf{V}_{\mathrm{L}}(x,y) = \mathrm{i}\omega\mathbf{V}_{\mathrm{R}}(x,y), \tag{2.10}$$

$$L_{\mathrm{T}}(x,y) = \begin{bmatrix} 0 & L_{\mathrm{q}}(x,y) \\ -L_{\mathrm{q}}(x,y) & 0 \end{bmatrix}, \tag{2.11}$$

$$L_{\mathrm{q}}(x,y) = \begin{bmatrix} 0 & \gamma & \dfrac{\partial}{\partial y} \\ -\gamma & 0 & -\dfrac{\partial}{\partial x} \\ -\dfrac{\partial}{\partial y} & \dfrac{\partial}{\partial x} & 0 \end{bmatrix}. \tag{2.12}$$